

Article

Mulberry Extract Upregulates Cholesterol Efflux and Inhibits p38 MAPK-NLRP3 Mediated Inflammation in Foam Cells

Yuting Liu¹, Kefan Wang², Shuofei Yang, Liming Lu^{2*} and Guanhua Xue^{1*}

¹ Department of Vascular Surgery, Renji Hospital, Shanghai Jiao Tong University School of Medicine, Shanghai 200127, China.

² Shanghai Institute of Immunology, Department of Immunology and Microbiology, Shanghai Jiao Tong University School of Medicine, Shanghai 200025, China

* Correspondence: lulunew2003@163.com (L.M.L.), Telephone: +86-13916235624; guanhuaXue@yeah.net (G.H.X.), +86-18918358101

Abstract: The accumulation of foam cells in arterial intima and the accompanied chronic inflammation are considered major causes of neoatherosclerosis and restenosis. However, both the underlying mechanism and effective treatment for the disease are yet to be uncovered. In this study, we combined transcriptome profiling of restenosis artery tissue and bioinformatic analysis to reveal that NLRP3 inflammasome is markedly upregulated in restenosis and that several restenosis related DEGs are also targets of mulberry extract, a natural dietary supplement used in traditional Chinese medicine to improve liver vitality. Further pathway enrichment analysis identified MAPK signaling pathway to be involved in the inflammatory response of foam cells. Consistently, immunofluorescence microscopy shows co-localization of NLRP3 with CD68+ macrophages. We then evaluated the efficacy of mulberry extract in inhibiting both the formation of foam cells and their inflammatory response. We demonstrated that mulberry extract suppresses the formation of ox-LDL induced foam cells, possibly by upregulating the cholesterol efflux genes ABCA1 and ABCG1 to inhibit intracellular lipid accumulation. In addition, mulberry extract dampens NLRP3 inflammasome activation by stressing the MAPK signaling pathway. Collectively, our mechanistic and functional studies unveil the therapeutic value of mulberry extract in neoatherosclerosis and restenosis treatment by regulating lipid metabolism and inflammatory response of foam cells.

Keywords: restenosis; foam cells; NLRP3 inflammasome; MAPK signaling pathway

1. Introduction

Endovascular therapy has broad applications in clinical diagnosis and treatment of cardiovascular diseases[1]. However, restenosis remains a major cause of target lesion failure after interventional therapy because 15.3% of patients with femoral popliteal artery disease develop in-stent restenosis after stent implantation [2] despite the rapid development of drug treatment and surgical technology.

Histology, angiography and intravascular imaging data all suggest that neoatherosclerosis is an important contributing factor for restenosis after vascular stent treatment [3]. Neoatherosclerosis is triggered by the activation of endothelial cells, followed by the recruitment of circulating monocytes which subsequently differentiate to monocyte-derived macrophages and then macrophages foam cells. Foam cells are characterized by high intracellular lipid content and usually reside in the intima of artery hyperplasia[4]. The late stage of neoatherosclerosis is accompanied by thin-walled fibrous atherosclerosis and lipid rich neointima [5]. Activated neointima cells secrete enzymes and chemicals that modify LDL, which in turn activate neointima cells and trigger various inflammatory signals[6]. Thus, neoatherosclerosis plaques are featured by inflammation and lipids metabolic disorder.

NOD [nucleotide oligomerization domain]-, LRR [leucine-rich repeat]-, and PYD [pyrin domain]-containing protein 3 (NLRP3) containing inflammasome is an important

part of innate immunity and plays essential roles in inflammation[7]. NLRP3 is a key component of this multi-protein complex because it interacts closely with apoptosis-related dot-like protein (ASC) and recruits the precursor of cysteinyl aspartate specific proteinase (caspase-1) [8]. Previous studies revealed elevated expression of the NLRP3 inflammasome in human atherosclerotic arteries[9]. In addition, a study from the Canakinumab Anti-Inflammatory Thrombosis and Outcomes Study (CANTOS) showed that inhibition of IL-1 β induced by NLRP3 inflammation reduces the incidence of atherothrombotic events and inflammation in patients after myocardial infarction[10], suggesting that NLRP3 inflammasome may be a promising therapeutic target for cardiovascular diseases including atherosclerosis and restenosis. However, the underlying mechanism remains unclear.

Foam cells play key roles in the development of neoatherosclerosis. They are macrophages with excessive influx of modified Low Density Lipoprotein (LDL) and high accumulation of cholesteryl ester [11]. This biological process can be reversed by cholesterol efflux which utilizes ATP binding cassette transporter A1 (ABCA1), ATP binding cassette transporter G1 (ABCG1) and scavenger receptor B1 (SR-B1) to transport excess intracellular lipids to liver for degradation [12]. A traditional Chinese medicine Yin-xing-tong-mai decoction (YXTMD) has been used to treat atherosclerosis by activating the PPAR γ -LXR α -ABCA1/ABCG1 pathway to enhance cholesterol efflux[13].

Mulberry extract, a nutrition-rich natural dietary supplement, has long been used in Chinese medicine[14]. It has been shown to reduce lipid oxidative stress, inflammation, and lipids accumulation in liver and help ameliorate lipid metabolism disorders in a non-alcoholic fatty liver rat model[15]. In addition, the ethanol extract of black mulberry reduces foam cell formation and inhibits the development of atherosclerotic plaque through the ox-LDL-PPAR γ -CD36 feed-forward cycle[16]. The total phenols and flavonoids in the ethanol extract of mulberry and its derivative components are sufficient to elicit protective effects on oxidative stress and inflammation of macrophages stimulated by lipopolysaccharide[17]. Mulberry extract also contains a high concentration of biologically active compounds such as anthocyanins and flavonols, which inhibit the expression of inflammatory mediators induced by lipopolysaccharide in RAW264.7 cells and reduce the secretion of pro-inflammatory cytokines such as interleukin (IL)-6 and tumor necrosis factor (TNF)- α [18].

In this study, we revealed that mulberry extract not only inhibits the formation of foam cells by upregulating the cholesterol efflux to inhibit intracellular lipid accumulation but also dampens NLRP3 inflammasome activation by stressing the MAPK signaling pathway. Collectively, our results underscore the therapeutic value of mulberry extract in restenosis treatment.

2. Materials and Methods

2.1. Reagents

DMEM medium, fetal bovine serum (FBS), 100u / ml penicillin and 100u / ml streptomycin were purchased from GIBCO company of the United States. Oxidized low density lipoprotein (China Yeasen biology, 20605es05). Cell counting kit-8 (CCK-8), DOJINDO, Japan; Oil red O powder (absin biology, ab42024259); Total RNA extraction kit, reverse transcription kit, RT qPCR Kit (Yeasen biology, 10606es60, 11141es60, 11202es080). Anti-nlrp3 antibody (Abcam, ab214185); anti rabbit LgG (CST, 7074s); anti-caspase-1 antibody (Abcam, ab138483), anti-il-1 β Antibodies (CST, 31202); anti-Phospho-p38 MAPK antibody(CST, 4511); anti-p38 MAPK antibody (CST, 8690).

2.2. Mulberry extract

The mulberry fruit is sorted, pressed and filtered. The residue is filtered through solvent extraction, the filtrate and the residue extract are combined and the finished product is concentrated (Zhejiang Zhenming Biotechnology Co., Ltd.).

2.3. Tissue collection

Arterial samples were taken from patients with amputation due to atherosclerotic disease, while control arteries were taken from healthy individuals after accidental amputation. All samples are from Shanghai Renji University School of Medicine and processed in the Biobank of Renji Hospital. All procedures were approved by the Research Ethics Committee of Renji Hospital.

2.4. Cell cultures

RAW 264.7 cells were purchased from the American Type Culture Collection (ATCC). Cells were cultured in DMEM (Gibco, USA) supplemented with 10% fetal bovine serum (FBS) (Gibco,USA) plus 1% streptomycin in a humidified incubator at 5% CO₂ air and 37 °C. When the cells grow to 80% ~ 90% of the area, subculture and reserve.

2.5. Quantitative reverse transcription PCR (RT-qPCR)

The total RNA of cells was extracted according to the instructions of Trizol kit, and the RNA concentration and A260 / A280 ratio were measured by nano drop2000. cDNA was obtained by reverse transcription kit; The amount of mRNA was measured by RT-qPCR kit, and 3 replicates were set in each group. Reaction conditions: pre denaturation at 95 °C for 10min, denaturation at 95 °C for 15s, annealing / extension at 60for 30s, a total of 40 cycles. use $\Delta\Delta$ CT to calculate the gene expression level. The specific formula is as follows: Δ Ct= Ct value of target gene - Ct value of GAPDH Gene; $\Delta\Delta$ Ct = experimental group Δ Ct control group Δ Ct; Relative gene expression in the experimental group = $2^{-\Delta\Delta Ct}$.

| Project | Forwad primer sequence (5' to 3') | Reverse primer sequence (5' to 3') |
|-----------|-----------------------------------|------------------------------------|
| β-actin | GAAATCGTGCGTGACATTAA | AAGGAAGGCTGGAAGAGTG |
| NLRP3 | CCATCGGCAAGACCAAGA | ACAGGCTCAGAATGCTCATC |
| Caspase-1 | CGTCTTGCCCTCATTATCTG | TCACCTCTTTCACCATCTCC |
| IL-1β | TACGAATCTCCGACCACCAC- TACAG | TGGAGGTGGAGAGCTTTCAG- TTCATATG |
| ABCA1 | GCTTGTTGGCCTCAGTTAAGG | GTAGCTCAGGCGTACAGAGAT |
| ABCG1 | GTGGATGAGGTTGAGACAGACC | CCTCGGGTACAGAGTAGGAAAG |
| SRB1 | CGAAGTGGTCAACCCAAACGA | CCATGCGACTTGTCAGGCT |
| ABCA1 | GCTTGTTGGCCTCAGTTAAGG | GTAGCTCAGGCGTACAGAGAT |
| ABCG1 | GTGGATGAGGTTGAGACAGACC | CCTCGGGTACAGAGTAGGAAAG |

2.6. Western blotting

The human artery or cultured cells were lysed in a lysis buffer containing RIPA and 1 mM PMSF for 30 min on ice. After centrifugation at 12,000 × g for 15 min at 4 °C, the supernatants were collected as total proteins in artery or cells. The protein concentrations were also determined with a BCA assay kit. Aliquots (50 μg) of protein samples were separated on 10 % SDS-PAGE and electro-transferred to polyvinylidene fluoride membranes. The PVDF membranes were incubated with primary antibodies overnight at 4 °C after being blocked with 5 % nonfat milk for 1h. The membranes were then washed with TBST (5 times, 3 min each) and incubated with secondary antibodies for 1 ~ 2 h at 37 °C. The protein bands were detected with an enhanced chemiluminescence system on Tanon 5200s. Densitometric analysis was conducted by ImageJ. Actin proteins were detected as a control.

2.7. Immunofluorescence

Tissue sections embedded in paraffin were cut into 4 μm sections, deparaffinized in xylene and rehydrated in graded alcohol solution. Slides were blocked with 5% (v/v) donkey serum for 30min. After washing with 1x PBS, cells were stained with rabbit anti-NLRP3 and rabbit anti-CD68 overnight at 4°C. After 3 washes in PBS, the immunoreactive products were visualized by incubation with an appropriate secondary antibody (1:400) and DAPI (1:500, Roche 216276) to visualize cell nuclei. Confocal microscopy was conducted using an Olympus CX31 confocal microscope.

2.8. Oil Red O (ORO) staining

Lipid content was histologically assessed using ORO staining. RAW264.7 cells were plated in 24-well plates and incubated with 50 $\mu\text{g}/\text{mL}$ ox-LDL with or without Mulberry extract for 24 h. The cells were washed two times with PBS slightly, fixed with 4% paraformaldehyde for 30 min, and then stained with filtered ORO solution (in a 6:4 ratio of 0.5% ORO in ddH₂O) for 60 min. Wash the cells with distilled water for 1-2 times, 1-2 minutes each time and rinse with 60% isopropyl alcohol. The lipid droplets in the macrophages was observed under the microscope and collected images.

2.9. Cell Counting Kit-8 analysis

The Cell Counting Kit-8 (CCK-8) assay was applied to measure cell viability. RAW264.7 cells were cultured in a 96-well plate at a cell density of 5000 cells/well for 24 hours. They were added with different concentrations of ox-LDL or different concentrations of mulberry extract. After incubating for 24 hours, 10 μL /well CCK-8 is dissolved in 90 μL /well culture medium, 100 μL /well CCK-8 working solution was added. The OD value at the wavelength of 450 nm was measured using the microplate reader 1 h later.

2.10. Cellular Cholesterol assay

Cells were grown in 6-well plate to approximately 2×10^6 cells. The cells were washed twice with PBS to remove medium serum and re-suspended in 0.1ml of lysate per 1×10^6 cells and incubated in room temperature for 10 minutes. Lysates were then heated at 70°C for 10 minutes followed by centrifugation at 2000g for 5 minutes at room temperature. Supernatant was used for enzymatic assay. Total cholesterol assay kit (E1015; Applygen Technologies Inc) and free cholesterol assay kit (E1016; Applygen Technologies Inc) was used in cellular cholesterol assay. Working solution was prepared by mixing reagent R1 with reagent R2 in a 4:1 ratio. Dilute 5 mM cholesterol standard with anhydrous ethanol to 2500, 1250, 625, 312.5, 156, 78, 39 $\mu\text{mol}/\text{L}$ and cover promptly. 190 μL of working solution was added to the microplate. To each microplate, 10 μL of each blank control solution (anhydrous ethanol), standard, and testing sample were added, respectively. Plates were sealed with membrane and incubated at 37°C for 20 minutes followed by spectrometry assay. OD value of each microplate was measured at wavelength of 550 nm. The cholesterol content was corrected for the concentration of protein per mg, and the standard curve was plotted and the sample concentration was calculated. Free cholesterol concentration was measured by Free Cholesterol Assay Kits. Cholesteryl ester content was determined by subtracting FC from total cholesterol. Each test was performed in triplicate.

2.11. Cell apoptosis analysis

Cell apoptosis was measured by using Annexin V-FITC/PI apoptosis detection kit (BD556547). After treatment for 24 h, cells were collected, washed with PBS and resuspended in binding buffer. Then, cells were incubated with 5 μL Annexin V-FITC and 5 μL PI for 15 min at RT in the dark. A flow cytometer was used to analyze cell apoptosis. The rate of apoptosis is expressed as the percentage of annexin V cells (Annexin V + PI-) that are individually stained.

2.12. Metabolomics analysis

Accurately weigh 25 mg of sample, and add 0.6 mL 2- chlorophenylalanine (4 ppm) methanol (-20 °C), vortex for 30 seconds in 2 mL EP tube. Then, add 100 mg glass beads, put them into the tissue grinder, and grind for 90 s at 60 Hz. Room temperature ultrasound for 15 min, 4 centrifugation at 12000 rpm at 4 °C for 10 min, take 300 µL supernatant and filter through 0.22 µm membrane, and add the filtrate into the detection bottle. Use the rest of the samples for LC-MS detection.

2.13. Statistical analysis

Used online bioinformatics tools provided by DAVID (<https://david-d.ncifcrf.gov/>).

Experimental data were presented as means ± SEM. *n* expresses the number of independent experiments or samples. Statistical analysis was performed by the one-way analysis of variance (ANOVA) with the significance level set at $p < 0.05$ (GraphPad Prism8).

3. Results

3.1. Increased expression of NLRP3 in vascular tissues in restenosis

To understand the unique transcriptional network in restenosis, we used RNA-seq analysis to compare the transcriptome of artery tissue from restenosis patients and healthy controls undergoing lower-limb amputation. The volcano map (Fig. 1A) shows a total of 3429 differentially expressed genes (DEGs) ($\log_{2}FC > 2$ and $P \text{ value} < 0.05$), among which 605 DEGs being up-regulated and 2824 DEGs down-regulated in restenosis patients compare to healthy control. Further Gene Ontology (GO) and Kyoto Encyclopedia of Genes and Genomes (KEGG) analyses on the DEGs (Fig. 1B and 1C) reveal enriched pathways in cytokine-cytokine receptor interaction and biological processes immune system process (highlighted in red box). Heat map shows genes in cytokine-cytokine receptor interaction, such as Interleukin-1 (IL-1), are upregulated (Fig 1D). IL-1 is a common pro-inflammatory cytokine that plays a key role in the innate immune response[19].

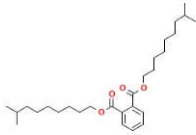
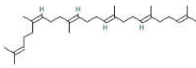
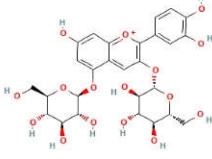
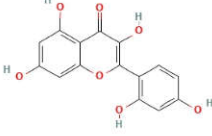
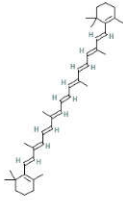
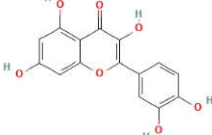
Since the NLRP3 inflammasome is an innate immune signaling complex and a key mediator of IL-1 family cytokine production[20], we tested its mRNA level in restenosis ($n=4$) and normal artery ($n=3$) tissues by RT-qPCR. The results show that NLRP3, caspase-1, and IL-1 β protein levels are all significantly up-regulated (Fig. 1E). Moreover, compared with normal control group, NLRP3 protein level also markedly increase in restenosis group shown by western blotting (Fig. 1F). Fluorescence in situ hybridization confirmed the elevated signal of NLRP3 in restenosis artery tissue accompanied by increase filtration of CD68+ macrophage. Importantly, the co-localization of NLRP3 and CD68 suggests that NLRP3 mainly expresses in neointima macrophages (Figure 1G). These results indicate a correlation between NLRP3 expression, especially in macrophages, and restenosis.

3.2. Active compounds in mulberry extract target genes involving in lipid metabolism and foam cell formation.

Mulberry leaf and fruit extracts have long been used as traditional Chinese medicines to improve liver health by regulating glucose and lipid metabolisms [21]. To evaluate the benefit of mulberry fruit extract in restenosis, we first tested its cytotoxicity on RAW264.7 macrophage. RAW264.7 cells were treated with different concentrations (0, 0.625, 1.25, 2.5, 5, 10mg/ml) of mulberry extract for 24 hours and the proliferation were measured by Cell Counting Kit-8 (CCK-8). We found that mulberry extract had no toxic effect on RAW264.7 cells up to the concentration of 10 mg/ml, (Fig. 2A). Therefore, all subsequent experiments used 10mg/ml as the highest concentration. Based on data obtained from the Traditional Chinese Medicine Systems Pharmacology Database (TCMSP: <http://tcmssp.com/tcmssp.php>), we identified six active compounds of mulberry extract with the criteria of OB $\geq 30\%$ and DL ≥ 0.18 (Table 1). In PubChem database, which provides information on the activities of chemical molecules in biological assays, we found 196 potential targets of these compounds. Next, we established a compound-target network using cytoscape to illustrate the interaction between these active compounds and their targets. Our network consists 203 nodes which represent active compounds or their

potential targets and 231 edges which indicate the interaction between the nodes (Fig 2B). These targets were compared with the 3429 DEGs, and 50 overlapping genes (Table 2) were chosen for further study to examine the mechanism and anti-restenosis efficacy of mulberry extract (Fig 2C). We also applied KEGG pathway enrichment (Fig 2D) and GO analysis (Fig 2E) on these anti-restenosis targets and found that they are mainly involved in biological processes related to lipid metabolism and atherosclerosis such as inflammatory response, negative regulation of lipid storage, and negative regulation of macrophage derived foam cell differentiation. We then used Cytoscape software to optimize and visualize the protein-protein interaction (PPI) network of these genes provided by the STRING database (<https://string-db.org/>). PPI is defined by interaction scores (medium: >0.4) (Fig 2F). Intriguingly, IL-1 β is one of the key hubs in the cluster (Table 3). The findings show that mulberry extract is non-toxic and could regulate inflammatory response and lipid metabolism in foam cells.

Table 1. The 6 active compounds of Mulberry.

| MOL ID | Name | MW | OB(%) | HL | Structure |
|-----------|--------------------|--------|-------|-------|---|
| MOL010300 | dIDP | 446.74 | 41.08 | 1.96 |  |
| MOL002372 | (E,E,E,E)-Squalene | 410.8 | 33.55 | 3.15 |  |
| MOL006209 | cyanin | 411.66 | 47.42 | 2.72 |  |
| MOL000737 | morin | 302.25 | 46.23 | 15.51 |  |
| MOL002773 | beta-carotene | 536.96 | 37.18 | 4.36 |  |
| MOL000098 | quercetin | 302.25 | 46.43 | 14.4 |  |

MW: molecular weight;OB: oral bioavailability; DL: drug-likeness

Table 2. 50 potential target genes of mulberry extract therapy for restenosis.

| No. | Target | Symbol | Entrez ID |
|-----|--|---------|-----------|
| 1 | Prostaglandin G/H synthase 2 | PTGS2 | 5743 |
| 2 | Prostaglandin G/H synthase 1 | PTGS1 | 5742 |
| 3 | Dipeptidyl peptidase IV | DPP4 | 1803 |
| 4 | Endothelin-1 | EDN1 | 1906 |
| 5 | Platelet glycoprotein 4 | CD36 | 948 |
| 6 | Vascular endothelial growth factor A | VEGFA | 7422 |
| 7 | Apoptosis regulator Bcl-2 | BCL2 | 596 |
| 8 | 72 kDa type IV collagenase | MMP2 | 4313 |
| 9 | Heme oxygenase 1 | HMOX1 | 3162 |
| 10 | Cytochrome P450 3A4 | CYP3A43 | 64816 |
| 11 | Cytochrome P450 1A2 | CYP1A2 | 1544 |
| 12 | Myc proto-oncogene protein | MYC | 4609 |
| 13 | Aldose reductase | AKR1B10 | 57016 |
| 14 | Potassium voltage-gated channel subfamily H member 2 | KCNH2 | 3757 |
| 15 | Sodium channel protein type 5 subunit alpha | SCN5A | 6331 |
| 16 | Gamma-aminobutyric acid receptor subunit alpha-1 | GABRA1 | 2554 |
| 17 | Proto-oncogene c-Fos | FOS | 2353 |
| 18 | Urokinase-type plasminogen activator | PLAU | 5328 |
| 19 | Matrix metalloproteinase-9 | MMP9 | 4318 |
| 20 | Pro-epidermal growth factor | EGF | 1950 |
| 21 | Interleukin-6 | IL6 | 3569 |
| 22 | NF-kappa-B inhibitor alpha | NFKBIA | 4792 |
| 23 | Hypoxia-inducible factor 1-alpha | HIF1A | 3091 |
| 24 | Cell division control protein 2 homolog | CDK1 | 983 |
| 25 | Cytochrome P450 1A1 | CYP1A1 | 1543 |
| 26 | Intercellular adhesion molecule 1 | ICAM1 | 3383 |
| 27 | Interleukin-1 beta | IL1B | 3553 |
| 28 | C-C motif chemokine 2 | CCL2 | 6347 |
| 29 | E-selectin | SELE | 6401 |
| 30 | Vascular cell adhesion protein 1 | VCAM1 | 7412 |
| 31 | Dual oxidase 2 | DUOX2 | 50506 |
| 32 | Nuclear receptor subfamily 1 group I member 2 | NR1I2 | 8856 |
| 33 | G2/mitotic-specific cyclin-B1 | CCNB1 | 891 |
| 34 | Thrombomodulin | THBD | 7056 |
| 35 | Arachidonate 5-lipoxygenase | ALOX5AP | 241 |
| 36 | Neutrophil cytosol factor 1 | NCF1 | 653361 |
| 37 | Hyaluronan synthase 2 | HAS2 | 3037 |

| | | | |
|----|---|--------|-------|
| 38 | C-X-C motif chemokine 2 | CXCL2 | 2920 |
| 39 | Nuclear receptor subfamily 1 group I member 3 | NR1I3 | 9970 |
| 40 | Peroxisome proliferator-activated receptor alpha | PPARA | 5465 |
| 41 | Peroxisome proliferator-activated receptor delta | PPARD | 5467 |
| 42 | Osteopontin | SPP1 | 6696 |
| 43 | Transcription factor E2F2 | E2F2 | 1870 |
| 44 | Purinergic receptor P2Y1 | P2RY6 | 5031 |
| 45 | Hypoxanthine-guanine phosphoribosyltransferase | HPRT1 | 3251 |
| 46 | Thymidylate synthase | TYMS | 7298 |
| 47 | Adenylate cyclase type 10 | ADCY10 | 55811 |
| 48 | Fructose-1,6-bisphosphatase | FBP1 | 2203 |
| 49 | Thymidine kinase, cytosolic | TK1 | 7083 |
| 50 | Cannabinoid receptor 2 | CNR2 | 1269 |

Table 3 Top 10 high degree genes in the PPI network.

| No. | Target | Symbol | Degree |
|-----|--------------------------------------|--------|--------|
| 1 | Interleukin-1 beta | IL1B | 30 |
| 2 | Interleukin-6 | IL6 | 29 |
| 3 | Prostaglandin G/H synthase 2 | PTGS2 | 28 |
| 4 | Vascular endothelial growth factor A | VEGFA | 28 |
| 5 | C-C motif chemokine 2 | CCL2 | 26 |
| 6 | Hypoxia-inducible factor 1-alpha | HIF1A | 25 |
| 7 | Epidermal growth factor receptor | EGF | 25 |
| 8 | Matrix metalloproteinase-9 | MMP9 | 25 |
| 9 | Myc proto-oncogene protein | MYC | 24 |
| 10 | Heme oxygenase 1 | HMOX1 | 23 |

3.3. Mulberry extract inhibits the expression of NLRP3 via the MAPK signaling pathway in foam cells

The accumulation of lipids in macrophages and foam cell formation are closely associated with the development of atherosclerosis[22]. In order to study the effect of mulberry extract on foam cell formation, we first established an in vitro inducible foam cell model[23]. Raw264.7 macrophages were induced with 50µg/ml oxidized low-density lipoprotein ox-LDL for 24 hours to form foam cells. We then used Oil Red O staining to detect the lipid droplets in cytoplasm, a major feature of foam cells, and found accumulation of intracellular lipid in induced cells (Figure 3A, compare left two panels). Increased intracellular cholesterol ester content (cholesterol ester = total cholesterol-free cholesterol) detected by the total cholesterol and free cholesterol enzyme quantification method further confirmed the successful formation of foam cells (Figure 3B). We then treated these ox-LDL-induced foam cells with either low (5mg/ml) or high concentration (10mg/ml) of mulberry extract for 24h to examine the intracellular lipid content using Oil Red O staining. Intriguingly, our results show that ox-LDL-induced foam cells treated with both high and low concentration of mulberry extract contain significantly less lipid droplets compared to the no-treatment cells (Figure 3A, compare right three panels). Consistently, the mulberry extract treated cells also show decreased levels of both total cholesterol and cholesterol ester (Figure 3B). We also observed that this inhibition is dose dependent (Figure 3B, compare lane 3 and 4). These results indicate that mulberry extract has the ability to inhibit ox-LDL-induced RAW264.7 macrophage foam cell production by suppressing intracellular lipid accumulation.

Since the lipid content of foam cells is associated with inflammation, we aimed to explore whether mulberry extract inhibits the inflammasome activity in these cells. To this end, we utilized the same ox-LDL-induced foam cells. After induction, we divided the cells into control, 1mg/ml, 5mg/ml and 10mg/ml mulberry extract treatment groups and proteins involved in inflammasome activity were detected by western blotting. Our results show that upon induction, the protein levels of NLRP3, caspase-1 and IL-β all markedly increased. In contrast, foam cells treated with mulberry extract show dosage dependent down-regulation of NLRP3, caspase-1, and IL-1β (Figure 3C).

Given that the MAPK signaling pathway plays essential role in various cardiovascular diseases and has been shown to regulate NLRP3 [24], we further explored the effects of mulberry extract on this pathway. GO analysis revealed that biological processes enriched in anti-restenosis targets are also involved in positive regulation of MAPK cascade and KEGG pathway enrichment analysis confirmed that MAPK signaling pathway is the principal pathway on these targets (Figure 2D-E). To test the efficacy of mulberry extract on MAPK pathway, macrophages were pretreated with mulberry extract for 1 hour, and

after ox-LDL induction, protein level of p38-MAPK and MAPK were determined by western blotting. The results demonstrate that cells treated with mulberry extract has reduced expression of p38-MAPK (Figure 3D). Therefore, mulberry extract may regulate NLRP3 inflammasome through p38 MAPK signaling pathway.

3.4. Mulberry extract stimulates cholesterol efflux and inhibits apoptosis of foam cells

To further understand the mechanism of mulberry extract, we applied liquid chromatography-mass spectrometry (LC-MS) based untargeted metabolomics analysis and identified 727 related metabolites. These metabolites and the anti-restenosis genes found in this study were then subjected to all pathways and metabolism pathways analysis by MetaboAnalyst (<https://www.metaboanalyst.ca/>) (Fig 4A-B). The results show that the ABC transporters pathway is among the top 20 most enriched pathways. ABCA1 and ABCG1 are members of ABC transporters and mediate cholesterol efflux[25]. Next, we used RT-qPCR to detect the transcriptional expression of ABCA1 and ABCG1 in ox-LDL induced foam cells with or without treatment of mulberry extract and found significant up-regulation of both ABCA1 and ABCG1 (Figure 4C). Our result suggests that mulberry extract may stimulate cholesterol efflux mediated by ABCA1 and ABCG1 in foam cells to suppress their lipid accumulation. We also evaluated the effect of mulberry extract on foam cell apoptosis by Annexin V flow cytometry. Compared to that of control group, treatment with 50 ug/ml ox-LDL for 24 h significantly increases the percentage of apoptotic cells. In contrast, we observed a dose dependent reduction of foam cell apoptosis with pretreatment of mulberry extract. The percentage of apoptotic cells drops from 32.1% in untreated cells to 24.2% in cells treated with 10 mg / ml mulberry extract (Figure 4D). The results altogether demonstrate the efficacy of mulberry extract in controlling cholesterol efflux and reducing apoptosis.

Figure1

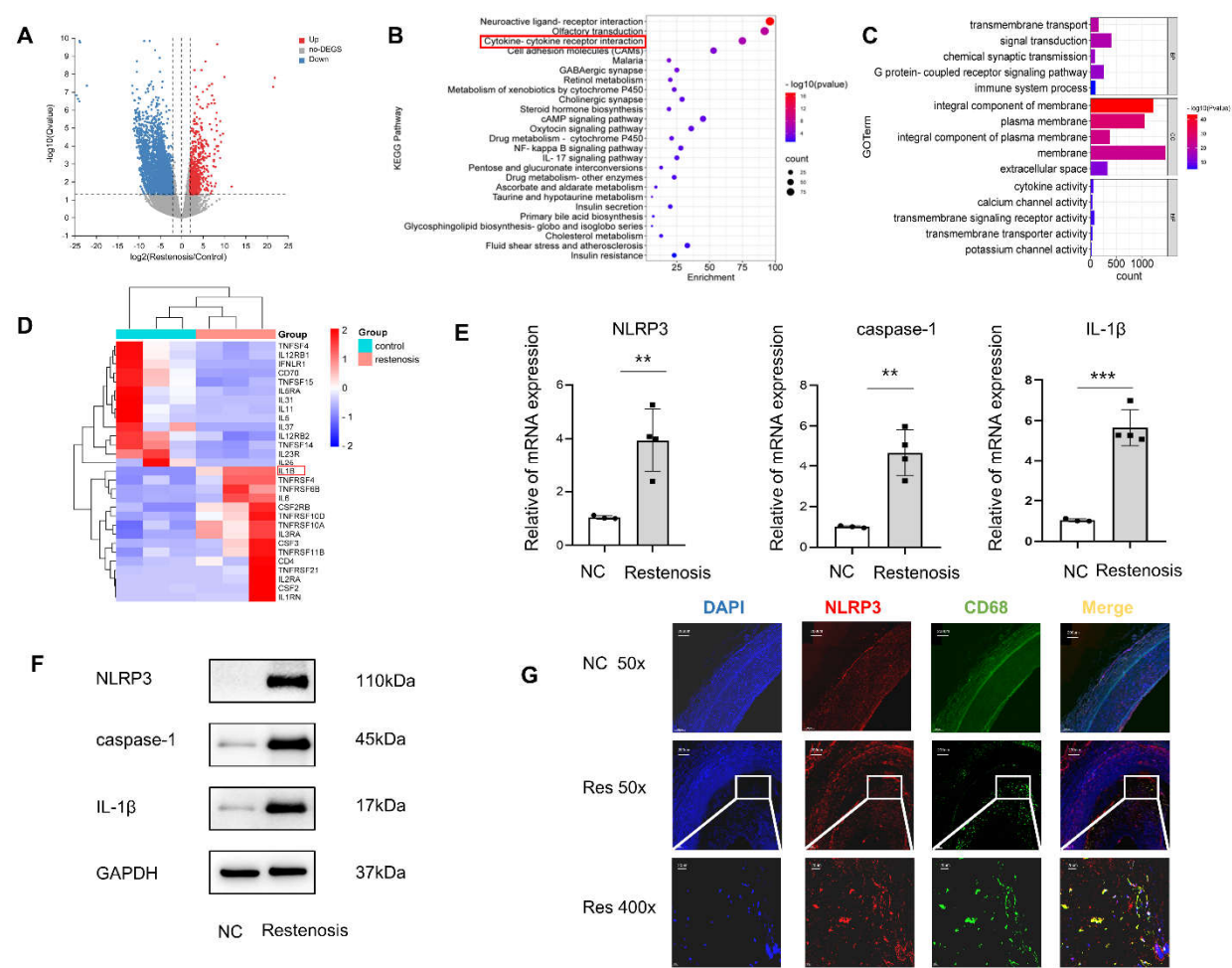


Figure 1. NLRP3 pathway is upregulated in neointima macrophages of restenosis patients. (A) Volcano plot (left) shows gene expression level in artery tissue of restenosis patients or healthy control with $-\log_{10}$ adjusted p-value (y-axis) versus \log_2 fold-change (x-axis). Up- and down-regulated DEGs (with adjusted p-value <0.05 and \log_2 fold-change >2) are labeled with red and blue dots, respectively. Genes with no significant change are labeled with grey dots. (B) KEGG pathway enrichment analysis of the DEGs reveals the top enriched biological processes in artery tissue of restenosis patients compared to healthy control. (C) GO enrichment analysis of DEGs (BP: biological process, CC: cellular component, and MF: molecular function). (D) Heat-map shows differentially expressed genes (with adjusted p-value <0.05 and \log_2 fold-change >2) between restenosis patients or healthy control (n=3). (E) The mRNA expression levels of NLRP3, caspase-1, and IL-1 β in artery tissue of restenosis patients or healthy control were validated by RT-qPCR. Relative expressions were normalized to β -actin (n=4 per group). (F) Protein expression of NLRP3, caspase-1, and IL-1 β were determined by western blotting. (G) Expression of NLRP3 and CD68 in normal and restenotic artery by immunofluorescence. Red, NLRP3; green, CD68; blue, DAPI nuclear staining. Compared with normal arterial tissue, **p<0.01, ***p<0.001. NC: Normal Control Res: Restenosis FC: Fold change.

Figure2

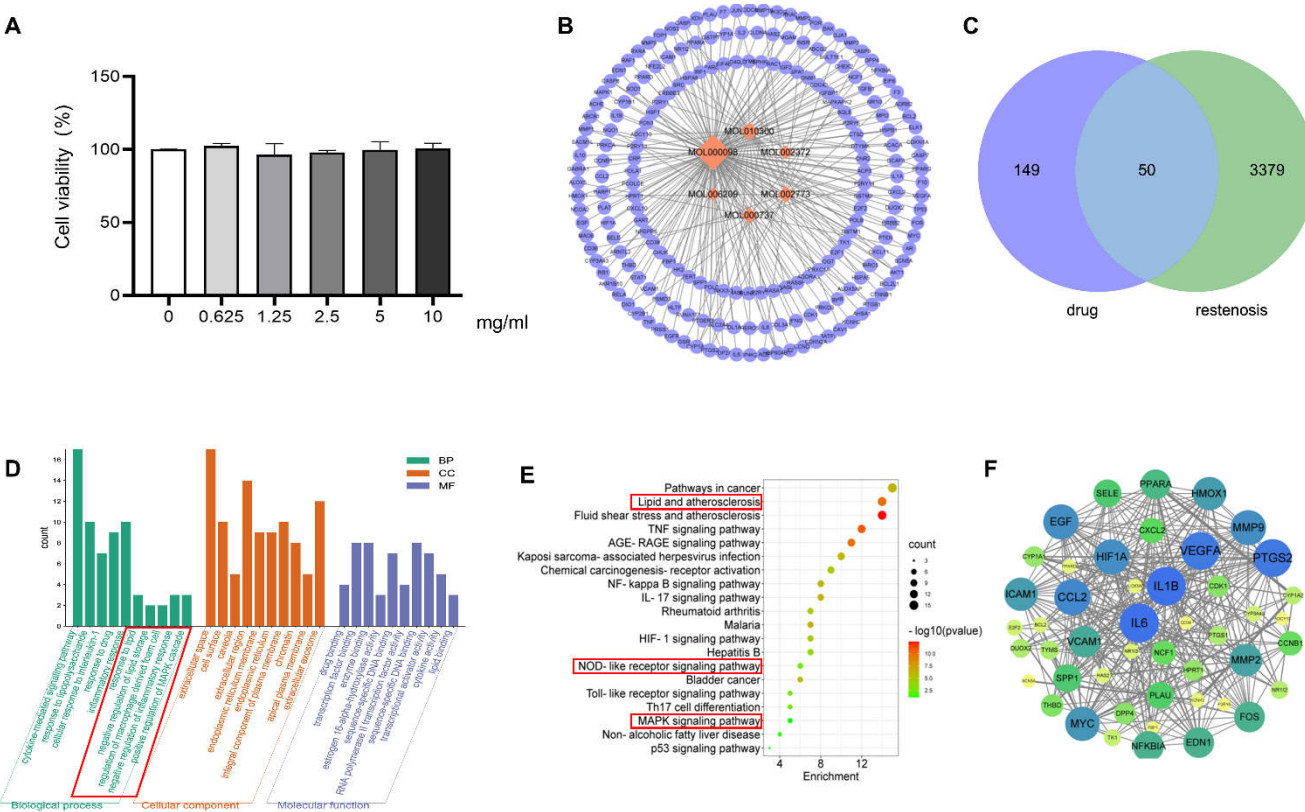


Figure 2. Active compounds of mulberry extract target anti-restenosis genes. (A) RAW 264.7 macrophages were treated with mulberry extract (0, 0.625, 1.25, 2.5, 5, and 10mg/ml) for 24h, and cell viability was measured by CCK-8 method. (B) Predicted network of targets of mulberry-derived compounds using Traditional Chinese Medicine Systems Pharmacology Database. Orange nodes represent the active compounds, purple nodes the predicted targets, and edges indicate the interactions between compounds and targets. The size of nodes is proportional to the degree of interaction. (C) Venn diagram shows overlapping genes of predicted targets of mulberry compounds and genes down-regulated in restenosis tissue. (D) KEGG pathway enrichment analysis and (E) GO enrichment analysis of the overlapping genes in (C). Pathways involve in lipid metabolism and inflammation are highlighted with red box. (F) Protein-protein interaction (PPI) network analysis of the overlapping genes by Cytoscape. Node size is proportional to the degree of interaction.

Figure3

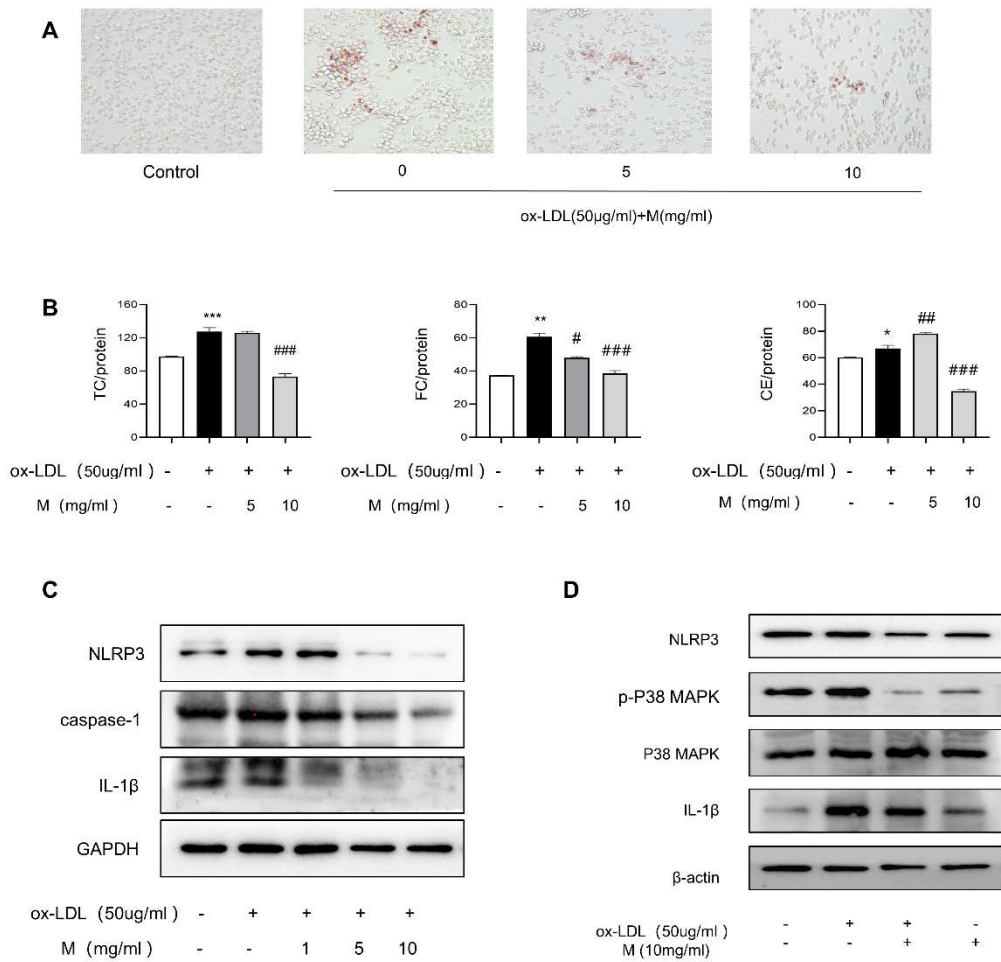


Figure 3. Mulberry extract inhibits the expression of NLRP3 in foam cells via MAPK signaling pathway. Foam cells were induced by treating RAW264.7 macrophages with 50 µg/ml ox-LDL for 24 hours. The cells were then given mulberry extract at low (5mg/ml) or high concentration (10mg/ml) as indicated. Following foam cell features were monitored. (A). Intracellular lipid level measured by Oil Red O staining. (B). Cholesterol ester content. (TC, total cholesterol; FC, free cholesterol; CE, cholesterol ester) qualified by Cellular Cholesterol assay of foam cells with or without treatment of mulberry extract as indicated. (C). Induced foam cells were treated with different concentrations of mulberry extract (0,1,5,10 mg/ml) for 24 hours and protein levels of NLRP3, caspase-1, and IL-1 β were determined by western blotting. (D) The protein levels of NLRP3, p-p38, p38 MAPK, and IL-1β protein levels of cells undergoing indicated treatments were determined by western blotting. Graph bars represent qualification of flow cytometry results (Data shown are mean ± SEM. Statistical significance was determined by two-way ANOVA with correction for multiple comparisons. *=p<0.01, **=p<0.001, ***=p<0.0001, ##=p<0.01 and ###=p<0.001).

Figure 4

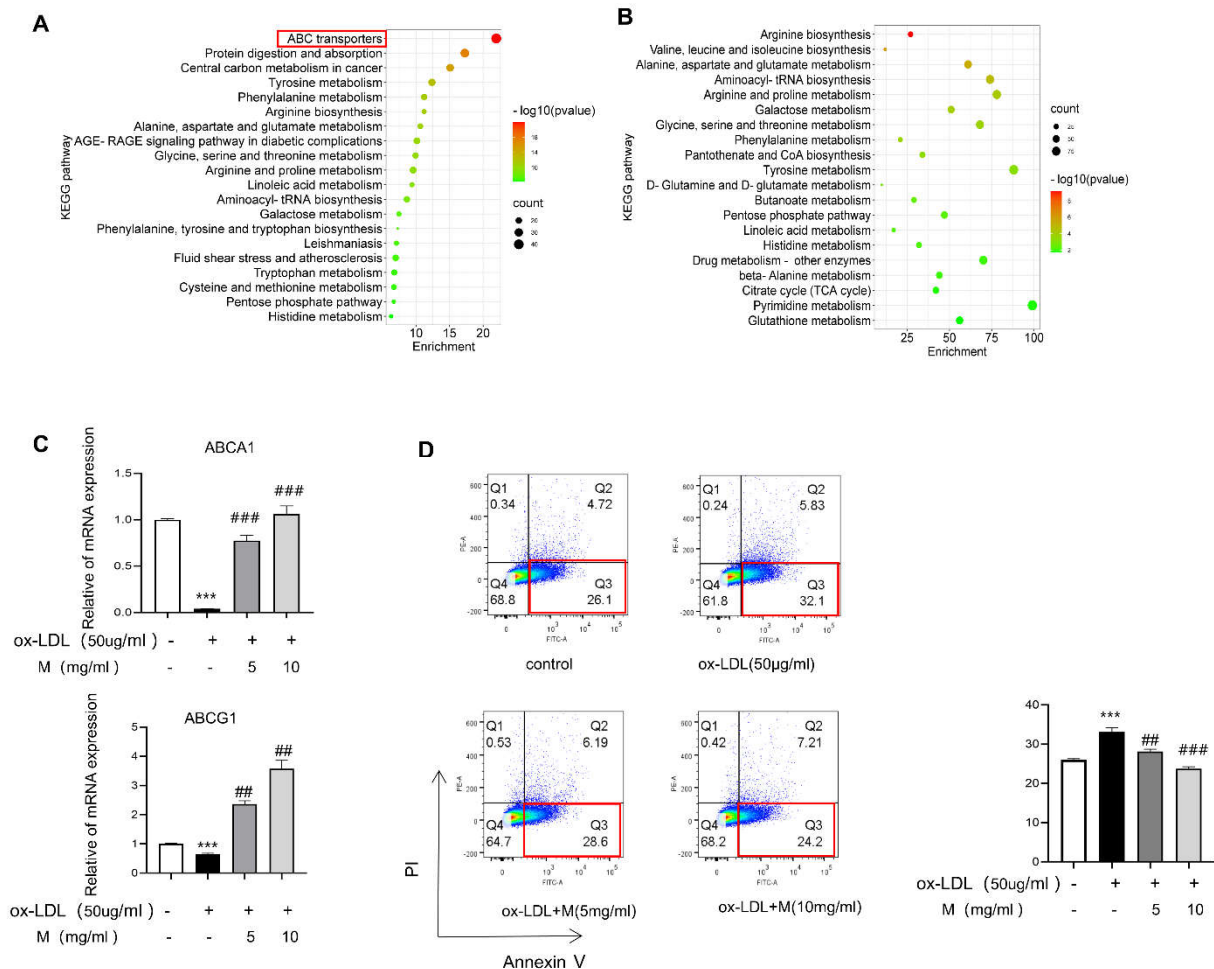


Figure 4. Mulberry extract treatment elevates cholesterol efflux and inhibits lipid accumulation and apoptosis in foam cells. (A) Pathways enrichment analysis of combined parameters of mulberry extract related metabolites and anti-restenosis genes identified in this study using MetaboAnalyst. Cholesterol efflux pathway is highlighted by red box. (B) Metabolism pathways analysis using MetaboAnalyst. (C) The mRNA expression levels of ABCA1 and ABCG1 in induced foam cells with or without mulberry treatment as indicated were validated by RT-qPCR. Relative expressions were normalized to β -actin gene. (D) Apoptosis of induced foam cells with or without mulberry treatment as indicated was detected using Annexin V flow cytometry (representative data are shown from 3 independent experiments). Graph bars represent qualification of flow cytometry results (Data shown are mean \pm SEM. Statistical significance was determined by two-way ANOVA with correction for multiple comparisons. ***=p<0.001, ****=p<0.0001, ##=p<0.01 and ###=p<0.001).

4. Discussion

Foam cells, a group of lipid rich macrophages, play essential roles in the development of restenosis. In this study, we found that mulberry extract, a natural dietary supplement used in traditional Chinese medicine, inhibits the formation of foam cells by stimulating the cholesterol efflux and provides a new therapeutic strategy for the treatment of restenosis. Our mechanistic studies by RNA-sequencing and network pharmacological analysis of overlapping genes regulated by both mulberry extract and restenosis reveal that the reduction of lipid deposition and attenuation of inflammation in foam cells may be the future directions for preventing restenosis and its clinical manifestations.

The main mechanical feature of restenosis after endovascular treatment is insufficient stent expansion or fracture. Meanwhile, local inflammation leads to invasive neointimal

hyperplasia and neoatherosclerosis[26]. During the development of restenosis, macrophages infiltrate in neointima and eventually aggregate near the surface of the stent and cause neoatherosclerosis that is not related to the original atherosclerotic tissue [27]. Subsequently, these fat-laden macrophages, or foam cells, form atherosclerotic plaques, which can evolve into thin-walled atherosclerotic plaques with the risk of plaque rupture and occasional calcification[27]. The transformation of macrophages into foam cells is characterized by lipid droplet formation and massive lipid accumulation [28]. To reverse this biological process, cholesterol transporters such as ABCA1 and ABCG1 mediate cholesterol efflux from macrophages to extracellular lipid acceptors. ABCA1 and ABCG1 deficiency increases foam cell formation and accelerates the development of atherosclerosis in mice. Several Chinese medicines are shown to promote cholesterol efflux by regulating the PPAR γ -LXR α -ABCA1/ABCG1 pathway including Chrysin[29], Yin-xing-tong-mai decoction[13] and Qing-Xue-Xiao-Zhi formula[30]. However, it is difficult to identify the active ingredient in these multi-ingredient medicines and their anti-inflammatory mechanism remains to be elucidated. Statins, as cholesterol-lowering drugs, are effective in reducing cardiovascular disease and mortality in patients at high risk of cardiovascular disease.[31] Nevertheless, it may cause side effects including rhabdomyolysis and liver dysfunction[32]. In contrast, mulberry is a nutrition-rich dietary source and mulberry extract has no adverse health effect on human. Mulberry has been used in traditional Chinese medicine for centuries and increasing number of recent studies also show that mulberry fruit or leaf extracts are effective in boosting immunity, lowering blood glucose and promoting metabolism[33]. Our results, for the first time, show that mulberry extract treatment increases the expression of cholesterol efflux genes ABCA1/ ABCG1 and inhibits lipid droplet formation and lipid deposition in foam cells. Interestingly, our metabolic pathway analysis of mulberry targets in restenosis related genes reveals a significant enrichment of arginine biosynthesis. L-arginine, as a substrate for intracellular NO synthesis, has a variety of biological functions such as improving endothelial dysfunction and treating atherosclerosis[34]. A study in diabetes shows that oral L-arginine promotes NO synthesis and enhances vascular function[35]. In the future, we will further explore the role of mulberry extract in improving the function of endothelial cells as a new avenue to treat restenosis.

There are studies indicate a link between lipid and inflammation [36]. The two factors may establish a positive feedback mechanism and synergistically contribute to disease progression. For example, lipid accumulation in Abca1/g1-deficient myeloid cells promotes the activation of NLRP3 inflammasome[25]. Abnormal lipid metabolism also causes increased expression of pro-inflammatory cytokines and activating inflammation in atherosclerotic plaques[37]. Our study used bioinformatic analyses of restenosis related genes and predicted mulberry extract targets to identify potential anti-restenosis genes regulated by mulberry extract. The most noteworthy of these targets include genes associated with inflammation such as IL-1 β , IL-6, CD36, HIF-1 α , MMP2, ICAM-1, VCAM-1, and VEGF. CD36 participates in phagocytosis of apoptotic cells, pathogen recognition, and regulation of low-density lipoproteins. It also contributes to inflammatory responses and thrombotic diseases[38]. MMP-2 is a multifunctional protein which expression is elevated in many cardiovascular pathologies (e.g. myocardial infarction, hypertensive heart disease) where tissue remodeling and inflammatory responses are perturbed[39]. Among the targets are also IL-1 β which plays important roles in angiogenesis by synergistically inducing the production of VEGF with TNF and IL6. The expression of IL-1 β is dependent on the activation of NLRP3 because NLRP3 inflammasome cleaves pro-caspase-1 into the active form caspase-1, thereby promoting IL-1 β maturation and secretion[40]. IL-1 β in turn regulates the initiation and amplification of inflammatory process. Intriguingly, our RNA-seq and florescent imaging data reveal not only the increased levels of IL-1 β and NLRP3 in restenosis artery tissue but also a co-localization of NLRP3 with CD68⁺ macrophages, suggesting the regulatory roles inflammasomes in foam cells play in the development of restenosis. We also found that mulberry extract is effective in suppressing the

activation of NLRP3 inflammasome. The mRNA and protein expression of NLRP3 in mulberry extract treated foam cells are significantly decreased in a dosage dependent manner, making mulberry extract a promising therapeutic treatment for restenosis patients.

Protein kinases, including JNK, p38 MAPK and ERK, are activated in response to various stresses[41]. P38 MAPK pathway is usually involved in stress and inflammatory response[42] and has been shown to regulate NLRP3 inflammasome activation[43]. From the database of traditional Chinese medicine, we found that multiple target genes of mulberry active compounds are involved in the MAPK signal pathway. We speculated that mulberry extract may regulate the activation of NLRP3 inflammatory bodies of macrophages via p38 MAPK pathway. Indeed, our data supports this hypothesis by showing that the protein levels of NLRP3, phosphorylated p38 MAPK, and IL-1 β all decrease upon treatment of mulberry extract, making mulberry extract a potential treatment for not only restenosis but also other inflammation related diseases.

In summary, our study uncovers the elevated expression of NLRP3 in restenosis artery wall, making it a novel therapeutic target for the disease. More importantly, we found that mulberry extract plays multiple regulatory roles in the formation of restenosis. It not only inhibits the inflammation in foam cells by suppressing p38 MAPK signaling pathway mediated inflammasome activation but also stimulates the ABCA1/ABCG1 mediated cholesterol efflux of foam cells to decrease their formation. Therefore, mulberry extract is a promising all natural and highly effective treatment for neoatherosclerosis and restenosis.

Author Contributions: Yuting Liu: Methodology, Data curation, Writing- Original draft. Kefan Wang: Methodology, Software, Validation, Formal analysis. Shuofei Yang: Visualization, Supervision, Software. Liming Lu: Conceptualization, Resources, Writing- Reviewing and Editing, Funding acquisition. Guanhua Xue: Writing- Reviewing and Editin, Funding acquisition. All authors have read and agreed to the published version of the manuscript.

Funding: This work was supported by the National Natural Science Foundation of China (No. 81873526, 82071856); The National Key Research and Development Program (2020YFA010045); Shanghai Municipal Commission of Health, Scientific Research Program of Traditional Chinese medicine (2020JP009)

Conflicts of Interest: The authors declare that they have no known competing financial interests or personal relationships that could have appeared to influence the work reported in this paper.

References

1. Sun Z. Endovascular stents and stent grafts in the treatment of cardiovascular disease. *J Biomed Nanotechnol.* 2014; 10: 2424-63.
2. Qato K, Conway AM, Mondry L, Giangola G, Carroccio A. Management of isolated femoropopliteal in-stent restenosis. *J Vasc Surg.* 2018; 68: 807-10.
3. Park SJ, Kang SJ, Virmani R, Nakano M, Ueda Y. In-stent neoatherosclerosis: a final common pathway of late stent failure. *J Am Coll Cardiol.* 2012; 59: 2051-7.
4. Funk JL, Feingold KR, Moser AH, Grunfeld C. Lipopolysaccharide stimulation of RAW 264.7 macrophages induces lipid accumulation and foam cell formation. *Atherosclerosis.* 1993; 98: 67-82.
5. Jinnouchi H, Kuramitsu S, Shinozaki T, Tomoi Y, Hiromasa T, Kobayashi Y, et al. Difference of Tissue Characteristics Between Early and Late Restenosis After Second-Generation Drug-Eluting Stents Implantation - An Optical Coherence Tomography Study. *Circ J.* 2017; 81: 450-7.
6. Pentikäinen MO, Oörni K, Ala-Korpela M, Kovanen PT. Modified LDL - trigger of atherosclerosis and inflammation in the arterial intima. *J Intern Med.* 2000; 247: 359-70.
7. Rathinam VA, Fitzgerald KA. Inflammasome Complexes: Emerging Mechanisms and Effector Functions. *Cell.* 2016; 165: 792-800.
8. Zhen Y, Zhang H. NLRP3 Inflammasome and Inflammatory Bowel Disease. *Front Immunol.* 2019; 10: 276.
9. Shi J, Guo J, Li Z, Xu B, Miyata M. Importance of NLRP3 Inflammasome in Abdominal Aortic Aneurysms. *J Atheroscler Thromb.* 2021; 28: 454-66.
10. Ridker PM, Everett BM, Thuren T, MacFadyen JG, Chang WH, Ballantyne C, et al. Antiinflammatory Therapy with Canakinumab for Atherosclerotic Disease. *N Engl J Med.* 2017; 377: 1119-31.
11. Javadifar A, Rastgoo S, Banach M, Jamialahmadi T, Johnston TP, Sahebkar A. Foam Cells as Therapeutic Targets in Atherosclerosis with a Focus on the Regulatory Roles of Non-Coding RNAs. *Int J Mol Sci.* 2021; 22.

12. Wang N, Westerterp M. ABC Transporters, Cholesterol Efflux, and Implications for Cardiovascular Diseases. *Adv Exp Med Biol.* 2020; 1276: 67-83.
13. Zheng S, Huang H, Li Y, Wang Y, Zheng Y, Liang J, et al. Yin-xing-tong-mai decoction attenuates atherosclerosis via activating PPAR γ -LXR α -ABCA1/ABCG1 pathway. *Pharmacol Res.* 2021; 169: 105639.
14. Jan B, Parveen R, Zahiruddin S, Khan MU, Mohapatra S, Ahmad S. Nutritional constituents of mulberry and their potential applications in food and pharmaceuticals: A review. *Saudi J Biol Sci.* 2021; 28: 3909-21.
15. Memete AR, Timar AV, Vuscan AN, Miere Groza F, Venter AC, Vicas SI. Phytochemical Composition of Different Botanical Parts of *Morus* Species, Health Benefits and Application in Food Industry. *Plants (Basel).* 2022; 11.
16. Liu YG, Yan JL, Ji YQ, Nie WJ, Jiang Y. Black mulberry ethanol extract attenuates atherosclerosis-related inflammatory factors and downregulates PPAR γ and CD36 genes in experimental atherosclerotic rats. *Food Funct.* 2020; 11: 2997-3005.
17. Yu JS, Lim SH, Lee SR, Choi CI, Kim KH. Antioxidant and Anti-Inflammatory Effects of White Mulberry (*Morus alba* L.) Fruits on Lipopolysaccharide-Stimulated RAW 264.7 Macrophages. *Molecules.* 2021; 26.
18. Jung S, Lee MS, Choi AJ, Kim CT, Kim Y. Anti-Inflammatory Effects of High Hydrostatic Pressure Extract of Mulberry (*Morus alba*) Fruit on LPS-Stimulated RAW264.7 Cells. *Molecules.* 2019; 24.
19. Dinarello CA. Interleukin-1 in the pathogenesis and treatment of inflammatory diseases. *Blood.* 2011; 117: 3720-32.
20. Grebe A, Hoss F, Latz E. NLRP3 Inflammasome and the IL-1 Pathway in Atherosclerosis. *Circ Res.* 2018; 122: 1722-40.
21. Lim HH, Lee SO, Kim SY, Yang SJ, Lim Y. Anti-inflammatory and antiobesity effects of mulberry leaf and fruit extract on high fat diet-induced obesity. *Exp Biol Med (Maywood).* 2013; 238: 1160-9.
22. Liu X, Guo JW, Lin XC, Tuo YH, Peng WL, He SY, et al. Macrophage NFATc3 prevents foam cell formation and atherosclerosis: evidence and mechanisms. *Eur Heart J.* 2021; 42: 4847-61.
23. Zhang C, Zhang X, Gong Y, Li T, Yang L, Xu W, et al. Role of the lncRNA-mRNA network in atherosclerosis using ox-low-density lipoprotein-induced macrophage-derived foam cells. *Mol Omics.* 2020; 16: 543-53.
24. Zhao W, Ma L, Cai C, Gong X. Caffeine Inhibits NLRP3 Inflammasome Activation by Suppressing MAPK/NF- κ B and A2aR Signaling in LPS-Induced THP-1 Macrophages. *Int J Biol Sci.* 2019; 15: 1571-81.
25. Westerterp M, Fotakis P, Ouimet M, Bochem AE, Zhang H, Molusky MM, et al. Cholesterol Efflux Pathways Suppress Inflammasome Activation, NETosis, and Atherogenesis. *Circulation.* 2018; 138: 898-912.
26. Shlofmitz E, Iantorno M, Waksman R. Restenosis of Drug-Eluting Stents: A New Classification System Based on Disease Mechanism to Guide Treatment and State-of-the-Art Review. *Circ Cardiovasc Interv.* 2019; 12: e007023.
27. Otsuka F, Byrne RA, Yahagi K, Mori H, Ladich E, Fowler DR, et al. Neoatherosclerosis: overview of histopathologic findings and implications for intravascular imaging assessment. *Eur Heart J.* 2015; 36: 2147-59.
28. Chistiakov DA, Bobryshev YV, Orekhov AN. Macrophage-mediated cholesterol handling in atherosclerosis. *J Cell Mol Med.* 2016; 20: 17-28.
29. Wang S, Zhang X, Liu M, Luan H, Ji Y, Guo P, et al. Chrysin inhibits foam cell formation through promoting cholesterol efflux from RAW264.7 macrophages. *Pharm Biol.* 2015; 53: 1481-7.
30. Li Y, Zhang L, Ren P, Yang Y, Li S, Qin X, et al. Qing-Xue-Xiao-Zhi formula attenuates atherosclerosis by inhibiting macrophage lipid accumulation and inflammatory response via TLR4/MyD88/NF- κ B pathway regulation. *Phytomedicine.* 2021; 93: 153812.
31. Robson J. Lipid modification: cardiovascular risk assessment and the modification of blood lipids for the primary and secondary prevention of cardiovascular disease. *Heart.* 2008; 94: 1331-2.
32. Ruscica M, Ferri N, Banach M, Sirtori CR, Corsini A. Side effects of statins-from pathophysiology and epidemiology to diagnostic and therapeutic implications. *Cardiovasc Res.* 2022.
33. Zhou M, Chen Q, Bi J, Wang Y, Wu X. Degradation kinetics of cyanidin 3-O-glucoside and cyanidin 3-O-rutinoside during hot air and vacuum drying in mulberry (*Morus alba* L.) fruit: A comparative study based on solid food system. *Food Chem.* 2017; 229: 574-9.
34. Li X, Gu J, Zhang Y, Feng S, Huang X, Jiang Y, et al. L-arginine alleviates doxorubicin-induced endothelium-dependent dysfunction by promoting nitric oxide generation and inhibiting apoptosis. *Toxicology.* 2019; 423: 105-11.
35. Kohli R, Meiningner CJ, Haynes TE, Yan W, Self JT, Wu G. Dietary L-arginine supplementation enhances endothelial nitric oxide synthesis in streptozotocin-induced diabetic rats. *J Nutr.* 2004; 134: 600-8.
36. Li Y, Schwabe RF, DeVries-Seimon T, Yao PM, Gerbod-Giannone MC, Tall AR, et al. Free cholesterol-loaded macrophages are an abundant source of tumor necrosis factor- α and interleukin-6: model of NF- κ B- and map kinase-dependent inflammation in advanced atherosclerosis. *J Biol Chem.* 2005; 280: 21763-72.
37. Westerterp M, Murphy AJ, Wang M, Pagler TA, Vengrenyuk Y, Kappus MS, et al. Deficiency of ATP-binding cassette transporters A1 and G1 in macrophages increases inflammation and accelerates atherosclerosis in mice. *Circ Res.* 2013; 112: 1456-65.
38. Silverstein RL, Febbraio M. CD36, a scavenger receptor involved in immunity, metabolism, angiogenesis, and behavior. *Sci Signal.* 2009; 2: re3.
39. Hardy E, Hardy-Sosa A, Fernandez-Patron C. MMP-2: is too low as bad as too high in the cardiovascular system? *Am J Physiol Heart Circ Physiol.* 2018; 315: H1332-h40.

-
40. Agostini L, Martinon F, Burns K, McDermott MF, Hawkins PN, Tschopp J. NALP3 forms an IL-1 β -processing inflammasome with increased activity in Muckle-Wells autoinflammatory disorder. *Immunity*. 2004; 20: 319-25.
 41. Kim EK, Choi EJ. Compromised MAPK signaling in human diseases: an update. *Arch Toxicol*. 2015; 89: 867-82.
 42. Coulthard LR, White DE, Jones DL, McDermott MF, Burchill SA. p38(MAPK): stress responses from molecular mechanisms to therapeutics. *Trends Mol Med*. 2009; 15: 369-79.
 43. Rajamäki K, Mäyränpää MI, Risco A, Tuimala J, Nurmi K, Cuenda A, et al. p38 δ MAPK: A Novel Regulator of NLRP3 Inflammasome Activation With Increased Expression in Coronary Atherogenesis. *Arterioscler Thromb Vasc Biol*. 2016; 36: 1937-46.

Graphical Abstract:

